JOURNAL OF GEOPHYSICAL RESEARCH, VOL. 99, NO. D4, PAGES 8257–8268, APRIL 20, 1994

Measurements of chloride depletion and sulfur enrichment in individual sea-salt particles collected from the remote marine boundary layer

L. M. McInnes,[1] D. S. Covert,[2] P. K. Quinn,[3] and M. S. Germani[4]

Abstract. Changes in the elemental ratios of Cl/Na and S/Na in sea-salt particles are expected from the atmospheric reactions of sulfuric and nitric acids with these particles. Chloride depletion is expected to occur upon the liberation of HCl to the gas phase, with the particles remaining enriched in sulfate or nitrate. The elemental ratios of Ca/Na, Mg/Na and K/Na should remain constant during this process. Analysis of chloride depletion and sulfur enrichment was obtained for individual sodium-containing particles from the remote marine Pacific atmosphere in both the accumulation mode ($0.06 \leq Dp \leq 1.0$ μm, where Dp is the particle diameter) and the coarse mode ($Dp > 1.0$ μm) size range. Sodium-containing particles comprised close to 100% of the coarse mode and 11 to 31% of the accumulation mode by number. Aerosols were collected with a low-pressure impactor and examined with a transmission electron microscope (TEM) coupled with an energy-dispersive X ray (EDX) detector. The elemental ratios obtained from the atmospheric particles were determined by comparison with values obtained from laboratory-generated sea-salt, sodium chloride, and sodium sulfate particles of known size and chemical composition, which served as a calibration set. The elemental ratios of Ca/Na, Mg/Na, and K/Na were found to remain fairly constant between individual sea-salt particles of various sizes for more than 85% of the particles examined. Deviations in the ratio of Cl/Na and S/Na from that of reference seawater values were observed most commonly for the submicrometer sea-salt aerosol. The Cl/Na ratio was significantly (Student's t test, 99.9%) lower than that of reference seawater for 89% of the particles examined, while the S/Na ratios were higher for 100% of the particles. The Cl/Na ratio measured in 48% of the coarse sea-salt particles ($1.0 < Dp \leq 2.5$ μm) reflected the ratio in bulk seawater, while the remaining particles had statistically lower ratios and qualitatively different morphologies. All but 3% of these coarse particles had enhanced S/Na ratios over that of bulk seawater. Estimates of non-sea-salt (nss) sulfate mass ranged from 216 to 1422 fg for particles of 0.50 μm in diameter to 861 and 5235 fg for particles of 0.80 μm in diameter, corresponding to 74 to 96% of the sea-salt particle mass. These values are compared with the recent measurements of *Mouri and Okada* [1993] as well as predictions from the atmospheric chemistry models of in-cloud sulfate production of *Hegg et al.*, [1992] and estimations of S(IV) oxidation in sea-salt aerosol water by *Chameides and Stelson* [1992].

Introduction

The aerosol in the marine boundary layer (MBL) results from two sources and a number of transformation processes which ultimately determine its size distribution with respect to number and chemical composition. These parameters determine physical and optical effects and chemical feedbacks. The ocean surface is a source of sea-salt particles which have a dominant mass mode greater than 1 μm and a significant tail in their number distribution extending to much smaller sizes that is not well quantified. The upper troposphere is a source of acidic sulfate aerosol [*Clarke*, 1992; *Raes et al.*, 1992] which is confined to sizes less than 0.5 μm on both a number and mass basis. This mixture is modified in the MBL by a number of processes, including uptake of $SO_2(g)$, deposition of condensable sulfate vapors, reactions with ammonia which occur in both clean air and clouds and cloud droplets.

Heightened interest in the chemical composition and chemical heterogeneity of ambient sea-salt particles [*Sievering et al.*, 1992] stems from their potential role in controlling heterogeneous sulfur oxidation in the MBL. The particle number concentration (N), size distribution, and chemical composition of existing sulfate particles are parameters used to model the number concentration of cloud condensation nuclei (CCN) and the light scattering coefficient of the aerosol population which relate to climatic effects [*Charlson et al.*, 1992]. Although sea salt does not normally contribute appreciably to the number concentration of CCN, measurements obtained from the Arctic [*O'Dowd and Smith*, 1993] under

[1]Department of Chemistry, University of Washington, Seattle.
[2]Joint Institute for the Study of Atmosphere and Ocean, University of Washington, Seattle.
[3]NOAA Pacific Marine Environmental Laboratory, Seattle, Washington.
[4]McCrone Associates, Westmont, Illinois.

Paper number 93JD03453.
0148-0227/94/93JD-03453$05.00

high wind speeds showed that the accumulation mode could at times be dominated by sea-salt particles. Sea-salt particles may actually form the seed for a large fraction of the CCN population on number (N) basis, while only a small fraction of the total CCN mass. Of interest is the relationship between the non-sea-salt (nss) sulfate to sodium mass ratio and the total number (N) to the sodium-containing number (N_{Na}) in the accumulation mode. Modeling results from *Hegg et al.* [1992] suggest that the number concentration and mean diameter of sea-salt particles available as CCN have a noticeable effect on in-cloud sulfate production. This translates to a large fraction of the new sulfate mass formed in-cloud being associated with these sea-salt particles. The resulting size distribution of the particle population which now contains significant excess sulfate would be shifted to larger sizes than the population expected to form without the presence of the sea-salt aerosol. The total number of new CCN would be less than the corresponding number formed in the absence of sea salt; however, at these larger sizes particles scatter light more efficiently and the increased sulfate production should translate to an increase in light scattering. In addition, below-cloud models of *Chameides and Stelson* [1992] predict a significant removal mechanism for $SO_2(g)$ from the scavenging of S(IV) gases by deliquescent sea-salt particles with subsequent oxidation to sulfate by $O_3(g)$. The extent of reaction is dependent on the sea-salt alkalinity with anticipated nss SO_4^{2-}/Na ratios around 0.005 (eq/eq). Since coarse sea-salt particles are removed fairly quickly from the lower atmosphere, this could represent a fast removal mechanism for $SO_2(g)$ and newly formed particulate sulfate and potentially a large mass flux of sulfate.

The reaction between sea salt and acidic nitrate and sulfate is expected to liberate HCl gas to the atmosphere leaving the particles enriched in nitrate and nss sulfate and depleted in chloride [*Eriksson*, 1959]:

$$HNO_3(g) + NaCl(p) \rightarrow HCl(g) + NaNO_3(p) \quad (1)$$

$$H_2SO_4(g) + 2NaCl(p) \rightarrow 2HCl(g) + Na_2SO_4(p) \quad (2)$$

On a molar basis the amount of chloride lost should be less than or equal to the nitrate and twice the sulfate added. In the remote marine Pacific atmosphere the concentration of aerosol nitrate is usually low [*Prospero et al.*, 1985]. Reactions between sea-salt and acidic sulfate would produce particles with molar ratios between that of unreacted sea salt (nss SO_4^{2-}/Na = 0) and fully reacted sea salt (nss SO_4^{2-}/Na = 0.59) where all the chloride has been replaced by sulfate. This neglects the possible contribution from gaseous ammonia. Depending on the ambient concentrations of reactant species and the atmospheric lifetimes of the sea-salt particles, the mass of sulfate measured on an individual particle could vary between sea-salt particles of different sizes as well as between sea-salt particles within the same size range. If the available time and surface area control the extent of reaction, smaller sea-salt particles which have higher average residence times and surface area to volume ratios than larger ones will show a higher proportion of chloride depletion and nss sulfate enrichment. The mass of the sea-salt cations, Na, Ca, Mg, and K, should be conserved throughout this process.

Field measurements conducted over the Atlantic [*Sievering et al.*, 1991, 1992] and the Pacific Ocean [*Quinn et al.*, 1993] showed that at times as much as half of the measured nss sulfate mass was associated with sea-salt particles larger than 0.9 μm. Correlations of gaseous HCl and sea-salt chloride depletion were obtained from bulk filter collections [*Keene et al.*, 1990] implying that sea-salt particles were the major source of volatile inorganic chlorine. The chloride deficits measured for the aerosols collected on bulk filters were too large to be explained simply by reactions of acidic nitrate and sulfate species alone, however [*Sievering et al.*, 1990]. Measurements from the coastal Atlantic [*Hitchcock et al.*, 1980], the remote tropical and equatorial Pacific [*Raemdonck et al.*, 1986], and the Arctic Ocean [*Shaw*, 1991] have shown chloride depletion on particles smaller than 4 μm, with the proportion of chloride depletion increasing with decreasing particle size. No significant fractionation of the seawater cations was found to occur. Other measurements from the remote Pacific have found the elemental ratios of Cl/Na similar to that of bulk seawater [*Parungo et al.*, 1986], while some bulk aerosol measurements on particles <1.1 μm have shown a chloride enrichment with respect to sodium [*Zhou et al.*, 1990].

The contribution of reacted sea-salt particles to the total aerosol number population and their chemical composition needs to be examined closely as a function of particle size and atmospheric lifetime to determine their role in the sulfate and number budgets of the MBL. As the extent of chemical reaction may vary from one particle to another, individual particle analysis is a useful approach, which can examine chemical variability between particles collected on short timescales, while bulk techniques can only provide an average chemical composition of the aerosol collected. *Mouri and Okada* [1993] reported measurements of elemental ratios with respect to sodium in individual sea-salt particles collected from the remote Pacific showing tremendous variability in the ratios of Cl/Na, S/Na, and also Ca/Na.

Here we report measurements from the MBL in the remote Pacific of individual sea-salt particle chemistry demonstrating the existence of sea-salt particles significantly depleted in chloride and enriched in non-sea-salt sulfate. Estimates of the abundance of sub-0.5-μm-diameter sea-salt-containing particles, sulfate particles, and sea-salt-containing particles which are completely depleted in chloride are made. These results are compared with those reported for sea-salt particles collected from the Pacific at 15°N by *Mouri and Okada* [1993] and with modeling predictions of in-cloud sulfate production by *Hegg et al.* [1992] and estimations of S(IV) oxidation in sea-salt aerosol water by *Chameides and Stelson* [1992].

Experiment

Aerosol Collection

Samples for individual particle analysis were collected during two separate field projects, the Pacific Sulfur Stratus Investigation (PSI-3) in the spring of 1991 and the International Global Atmospheric Chemistry Program's (IGAC) Marine Aerosol and Gas Exchange (MAGE) Pacific experiment in the spring of 1992. A low-pressure impactor (LPI) (PIXE Corporation International, Tallahassee, Florida) was used for separation of the coarse ($2.0 < Dp \leq 8.0$ μm, where Dp is the particle diameter) and sub-2.0-μm ($0.06 \leq Dp \leq 2.0$ μm) particles utilizing the corresponding stages. The flow rate of the impactor, 1.3 L/min, was controlled by a critical orifice. Carbon-coated transmission electron microscope (TEM) grids were mounted on stage inserts and positioned at a fixed distance directly under the jet of the corresponding

stage of interest. Collection times were pre-determined based on the ambient particle concentration (Dp > 14 nm) and ranged from a few minutes for the sub-2.0-μm aerosols to 1 hour for coarse particles. Samples were desiccated prior to examination with the electron microscope. No attempt was made to protect against the possibility of ammonia uptake by acidic particles during handling since the X ray analysis could not detect the presence of nitrogen species. The morphology of the nonvolatile acids is characteristic upon sampling and remains even after the particles absorb ammonia during handling [*Frank and Lodge*, 1967]. A brief description of the sampling strategy used in each field experiment follows.

PSI-3

Ambient samples were collected in April 1991 with the LPI mounted in situ from a 7-m tower at the University of Washington Cheeka Peak Research Station (480 meters (asl)). The station is located on the Olympic peninsula 2 km inland of the Washington coast (Figure 1) at 48°18′N and 124°37′W. Sample collection occurred when the onshore wind speed was greater than 2 m s^{-1} and the total particle count (Dp > 14 nm) was below 1000 particles cm^{-3}. No samples were collected when the tower was in cloud or fog or during precipitation events. A total of 25 grids were collected during a 2-week period for examination and analysis of the sub-2.0-μm particle population.

IGAC/MAGE

Additional samples were collected in February and March 1992 on a NOAA research cruise between Los Angeles, California and the equatorial Pacific (Figure 1). Sampling occurred during the N to S and S to N transits between Los Angeles and 12°S 135°W and for two time series stations at 12°S 135°W (7 days) and 2°S 140°W (2 days). Ambient samples were collected with the LPI in situ from a mast located 18 m above sea level with the ship directed into the wind. Samples were also collected off an inlet maintained at 25% relative humidity (RH) through a sampling port 7 m from the top of the mast. The particles were collected only for comparison purposes of particle morphology to those collected at ambient RH (typical range of 60–85%). No apparent difference in morphology was noted for the generally hygroscopic marine particles. This is expected due to the large pressure drop occurring across the stages of the impactor which effectively dries the particles before impaction. A total of 65 grids were collected with subsequent analysis of the sub-2.0-μm ($0.06 \leq Dp \leq 2.0$ μm) and the coarse ($2.0 \leq Dp \leq 8.0$ μm) particles. More than half of the grids originated from the two time series stations.

Electron Microscope Examination

The grids were previewed and photographed using a JEOL-100B transmission electron microscope (TEM) for the follow-

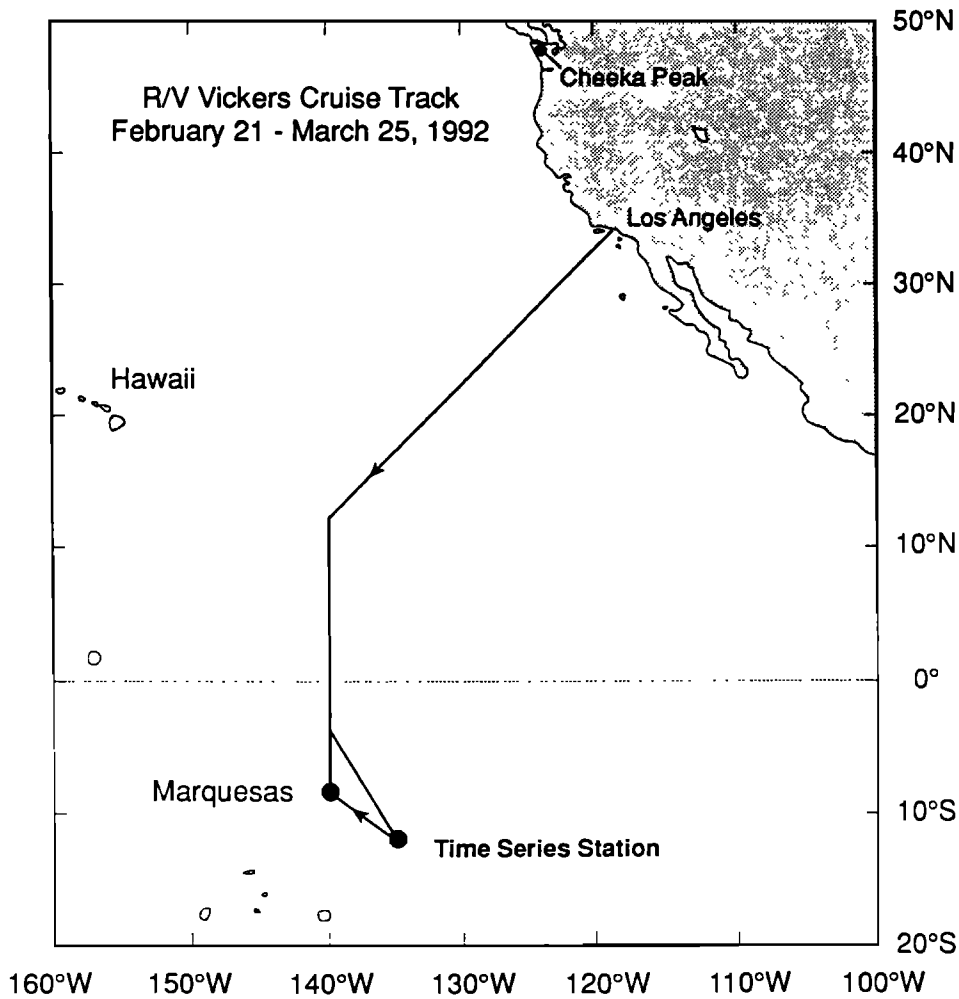

Figure 1. IGAC/MAGE equatorial Pacific field study.

ing parameters: particle size, characteristic morphology, and evidence of chemical heterogeneity and reacted particle types. Size measurements were calibrated with TEM micrographs of a carbon grating replica (E. F. Fullam). The size of a spherical particle was approximated by its diameter (*Dp*). For nonspherical particles, such as cubic salts, the size was estimated by averaging the diameter along two dimensions when the difference between the two lengths did not exceed 20%. For very irregular particle shapes, such as soot and oblong particles, no accurate size estimates were made. Instead, the longest and shortest dimensions were averaged. Irregular particle types did not significantly contribute to the total number concentration of the population described. Size distributions for the aerosol population between 0.02 μm and 9.6 μm were measured in the field using a differential mobility analyzer (DMA) (TSI model 3071, ThermoSystems Incorporated, St. Paul, Minnesota), particle counter (TSI model 3760), and an aerodynamic particle sizer (TSI model 3300) using the methods outlined by *Covert et al.* [1992]. Size distributions obtained using single-particle techniques were estimated only for comparison purposes to those obtained in the field, since in the high-vacuum environment of the electron microscope some volatile species are destroyed.

Information concerning the chemical composition of ambient aerosols in the marine boundary layer was inferred from the particle morphology coupled with information obtained from energy dispersive X ray analysis (EDX) and bulk size segregated chemistry obtained from ion chromatography. Characteristic satellite halos surrounding a particle indicate the presence of a nonvolatile acid [*Frank and Lodge*, 1967]. For sulfur-containing particles a distinction among ammonium sulfate, ammonium bisulfate, and sulfuric acid was made based on the number of satellites surrounding the particle [*Ferek et al.*, 1983]. Sea-salt particles, soot, and minerals were recognized by their characteristic morphology and relative stability under the conditions of induced heating from prolonged electron bombardment. When coupled with the EDX spectra, identification of the various types could be made. The stability of sodium sulfate particles was similar to that of sea-salt particles. Heterogeneous particles could usually be distinguished by compositional differences and apparent irregularities within an otherwise homogeneous composition. Reacted sea-salt particles were recognized by an apparent coating surrounding a particle core of recognizable morphology or a morphology different from that of the pure component. X ray analysis which revealed elemental spectra and ratios significantly different from that of the pure components later confirmed the existence of these mixed particle types.

Energy-Dispersive X ray Analysis

X ray spectra for elements with Z > 5 were collected at McCrone Associates (Westmont, Illinois) using a JEOL-2000 FX TEM equipped with an EDX detector (NORAN Z-max 30, Middleton, Wisconsin) for the particles obtained during PSI-3. The operating conditions of the electron beam during analysis were 200-keV accelerating potential with a filament current of 104 μA. X ray spectra were acquired for 60 live seconds from an area slightly larger than the entire particle. Information on chemical heterogeneity was obtained from selected area analysis where the X rays were generated within an area smaller than the entire particle so that chemically distinct areas were isolated for qualitative identification. Whole area analysis was used to obtain better estimates of the elemental ratios in heterogeneous particles. Spectra collected from the TEM grid and supporting film were obtained to determine their contribution to the background X ray signal. For this reason only qualitative identification of Si and C was possible, and even then only when the total counts for each element exceeded the average background counts by at least a factor of 3. Since laboratory aerosols were not available at the time of analysis of the PSI-3 data set, the elemental ratios of unreacted field particles substituted as a reference value. Unreacted field particles were chosen based on morphological information and X ray diffraction patterns taken of the major cubic crystalline portion. EDX analysis performed later using laboratory-generated particles of sea salt and sodium sulfate suggested that the reference values used for Cl/Na and S/Na were appropriate (agreement within 10%).

The samples collected during the IGAC/MAGE experiment were analyzed at the University of Washington using a JEOL-1200EX TEM with a NORAN Microtrace detector (Z > 10) with operating conditions of 120-keV accelerating potential and a filament current of 84 μA. X ray spectra generated from the entire particle area were collected for 60 live seconds. Additional X ray analysis was also obtained from selected areas of particles to distinguish regions of chemical heterogeneity within the particles. The laboratory particles used for the calibration sets in this case were artificial sea salt, sodium chloride, and sodium sulfate. The particles were generated from salt solutions (1–2% wt/wt) with a constant output atomizer (TSI model 3076). Once dried, they were sized (DMA, TSI model 3071) and impacted onto TEM grids. X ray analysis was performed under the same operating conditions and within a few hours of the atmospheric particles to duplicate the conditions of analysis as closely as possible.

Cliff-Lorimer [*Cliff and Lorimer*, 1975] sensitivity factors, k_{AB}, were estimated for each of the detectors where C_A and C_B were the concentrations of element A and

$$k_{AB} = \frac{C_A}{C_B} \times \frac{I_B}{I_A} \tag{3}$$

element B in the particle. The total X ray counts obtained for element A and element B are represented by I_A and I_B. The effects of absorption and fluorescence were ignored for the particles less than 1.0 μm given the low average atomic number (Z) and sizes of the particles examined. The values for I_B/I_A for the calibration particles were obtained from the slope of the regression lines from the calibration curves. The values for C_A and C_B were obtained for Na, K, Mg, Ca, Cl, and S (as SO_4^{2-}) on bulk filter collections of generated laboratory aerosol by ion chromatography (IC) (Dionex 2021i, Sunnyvale, California). The calculated Cliff-Lorimer values are estimated for both detectors in Table 1. The sensitivity of the X ray detector for low-Z elements is affected by window thickness and composition. The detector used for the PSI-3 data set at McCrone Associates, which has a window more transparent to lower-energy X rays, is more sensitive for Na. Due to the differences in detector sensitivity the results are shown separately for each detector.

The elemental ratios for individual sea-salt-containing particles were examined with respect to one of the conservative elements in sea salt. Sodium was the element chosen because its concentration is an order-of-magnitude larger than those of magnesium, calcium, or potassium. Of particular interest are the comparisons of the Cl/Na and S/Na ratios between ambient sea-salt-containing particles collected in the

Table 1. Experimentally Measured k_{AB} Values

Element A	Energy, keV	Artificial Sea Salt, k_{ANA}		NaCl	Na_2SO_4, k_{ANA}	
		d1	d2	d1	d1	d2
Na	1.03	1.00	1.00			
Mg	1.26	0.47	1.58			
Cl	2.63	0.35	1.21	0.33		
K	3.31	0.36				
Ca	3.69	0.25	1.32			
S	2.30	0.41	1.34		0.34	0.91

k_{AB}, Cliff-Lorimer sensitivity factors for element A with respect to element B.
d1, Noran microtrace ($Z > 10$); d2, Noran Zmax ($Z > 3$).

field, laboratory-generated sea salt, and sodium chloride particles of known chemical composition, and laboratory-generated sodium sulfate particles of known chemical composition. The variability in Ca/Na, Mg/Na, and K/Na ratios were also examined. The sulfur present in methanesulfonic acid (MSA) cannot be discerned from the sulfur present in sulfate by X ray techniques. From the size-segregated impactor measurements of aerosol concentrations made at Cheeka Peak, the MSA/non-sea-salt sulfate weight ratio was on average less than 0.07, showing maximum values in the size range 1.0 to 2.0 μm and 2.0 to 4.0 μm [*Quinn et al.*, 1993]. The contribution from MSA was assumed therefore to be small for the particle sizes examined.

The relative weight ratios of nss S/Na in sea-salt-containing particles were calculated by subtracting the seawater S/Na ratio (0.084, CRC Handbook of Chemistry and Physics, 1986) from the measured S/Na weight ratio determined by EDX. Individual particle mass, m, was inferred from the particle diameter, d, and particle density, ρ, using equation (4). The particle density was approximated by the density of sodium chloride

$$m = \frac{\pi}{6} d^3 \times \rho \tag{4}$$

(2.17 g cm^{-3}, CRC 1986). The mass of sodium in each sea-salt particle was estimated from the individual particle mass and the abundance of sodium in seawater, assuming no chemical fractionation occurs upon production. Sulfur mass was calculated based on S/Na weight ratios obtained from EDX analysis, multiplied by the estimated sodium values. Quantitative estimates of the fraction of nss sulfate mass contained in each particle was made assuming all the sulfur was sulfate. Quantitative estimates were not made based only on the total elemental counts for sulfur, due to the variation in net elemental counts for a particular element for sequentially analyzed particles of the same size. The relative ratios between elements of these same particles nevertheless are reproducible and it is for this reason that the relative ratios are presented.

Laboratory-Generated Aerosols

Laboratory aerosols were atomized from solutions of ammonium bisulfate, ammonium sulfate, artificial seawater, seawater collected from the time series station at 12°S 135°W, sodium sulfate, sodium chloride, and sodium methanesulfonate with a constant output atomizer (TSI model 3076). The aerosol size was selected with an electrostatic classifier and then impacted onto TEM grids using the low-pressure impactor. The diameters estimated from the TEM photographs were compared to the size selected from the DMA. Table 2 compares the particle size selected from the DMA with its apparent size on the grid. It can be seen that the geometric diameters of the impacted aerosol agree within 5 to 20% of the Stokes diameters selected using the DMA. Ion chromatography analysis of laboratory solutions and the bulk aerosols generated from these solutions was performed, and both results agreed well. Laboratory particles were generated at sizes of 0.15, 0.25, 0.50 μm and used as a calibration set for field particles up to sizes of 1.0-μm dry aerosol diameter. At least 10 particles of each of the sizes mentioned were used to generate the calibration curves. With increasing particle diameter ($Dp > 1.0$ μm) the effect of reabsorption of the lower-energy X rays such as Na could become significant. Until calibration aerosols are examined for particles of these sizes, the variability in the relative ratios for particles significantly larger than 1.0 μm is subject to a larger error.

Duplicate spectra were collected from the same sea-salt and sodium sulfate particles to ensure that any evaporative losses were not preferentially removing one of the elements of interest. For sequentially analyzed spectra, collected for 60 live seconds, the agreement was within 2% for Cl/Na and S/Na ratios. To determine if the relative ratios of the field particles were statistically different than the elemental ratios of the seawater reference value, a double-tailed Student's t test was applied. The confidence intervals were determined at 99.9% for the reference values. Sea-salt particles falling within this confidence interval were determined to have the same elemental ratios as bulk seawater. Values which fell outside of this interval had elemental ratios which were significantly different than bulk seawater ratios.

Results

Particle Morphology

The typical particle morphologies observed from samples collected both at Cheeka Peak and the equatorial Pacific can

Table 2. Comparison of Generated Aerosol Size Versus Impacted Aerosol Size

Aerosol	Size, μm	
	DMA	EM
Sodium chloride	0.20	0.20
Artificial seawater	0.20	0.21
12°S seawater	0.20	0.20
Sodium sulfate	0.20	0.21
Ammonium sulfate	0.20	0.20
Sodium methanesulfonate	0.20	0.20
Ammonium bisulfate	0.28	0.33*

* Error due to size estimates from photographs ±0.02 μm.

be grouped as ammonium sulfates and acidic sulfates (Figure 2), sea-salt particles with Cl/Na ratios close to bulk seawater (Figure 3), and sea-salt particles with Cl/Na ratios different than bulk seawater (Figures 4b and 4c). A subset of the sulfates consisted of mixed particles of sea salt and sulfate with diameters less than 0.5 μm (Figure 2). Selected area X ray analysis of these particle types determined that these electron dense inclusions contained the major elements present in sea salt: Na, Mg, Ca, K, as well as the presence or absence of Cl. Other mixed particles observed were larger sea salts with visually apparent coatings containing sulfur (Figure 5). Some of the sea-salt particles ($Dp \leq 2.0$ μm) collected during IGAC/MAGE were surrounded by a characteristic acidic halo (Figure 6), indicating the particles were acidic upon collection. Other sea-salt particles from the equatorial Pacific exhibited a morphology not typical of sea salt which revealed nss sulfur enrichments and depleted or nonexistent levels of chloride. An example of the transition in morphology which is believed to occur as the sea-salt particles are enriched with sulfur is shown (Figures 4a, 4b, and 4c). Figure 4a illustrates typical coarse sea-salt particle morphology observed during the 12°S time series station. As the particles accumulate higher loadings of sulfur (assumed to be sulfate), their morphology resembles that of Figures 4b and 4c. Figure 4c illustrates sea-salt-containing particles from a particularly interesting time period where both the morphology and the Cl/Na ratios changed noticeably from a morphology and chemical composition similar to sea salt (Figure 4a) to a morphology not typical of sea salt with a lower Cl/Na and higher S/Na ratio.

Elemental Composition

The results obtained from samples collected during PSI-3 showed varying molar ratios of Cl/Na and S/Na for sodium-containing particles of $Dp \leq 2.0$ μm (Figure 7). These particles are assumed to originate from sea salt since no other source of sodium is expected to contribute appreciably to this size range at this location. The EDX spectra of these particles also reveals additional sea-salt elements to confirm the sodium is from sea salt. The particle morphology was typical of sea-salt particles for most cases, except when small sea-salt inclusions were noticed within an ammonium sulfate or acidic sulfate particle ($Dp < 0.8$ μm). The Cl/Na, S/Na, and nss S/Na molar ratios were calculated from the background-corrected elemental ratios of X ray counts using equation (3). Many of the sea-salt particles (42%) are significantly (double-tailed t test, 99.9%) depleted in chloride by comparison to the reference sea-salt particle value. These same particles show sulfur enrichment although the S/Na ratio is less than one would obtain from a sea-salt particle in which the NaCl has been fully reacted with sulfate (0.59). Particles which show low Cl/Na values and fairly low S/Na values may illustrate the case where another source of acid was available besides sulfuric acid, or where another mechanism is controlling the chloride volatilization.

The data sets obtained for particles collected during IGAC/MAGE utilized laboratory-generated particles of known composition as calibration sets. Examples of the calibration curves obtained using the JEOL-1200FX for S/Na, Mg/Na, K/Na, and Ca/Na are shown in Figures 8a, 8b, 8c and 8d for particle sizes of 0.15, 0.25, and 0.50 μm. At least 10 particles from each size class were analyzed. For artificial sea-salt particles which crystallize into distinct pure phases upon drying, whole area analysis was considered the best method for obtaining accurate estimates of Ca/Na, Mg/Na, K/Na, and S/Na. Good correlation was found for each of the elements with respect to Na with regression coefficients $R^2 > 94\%$. For

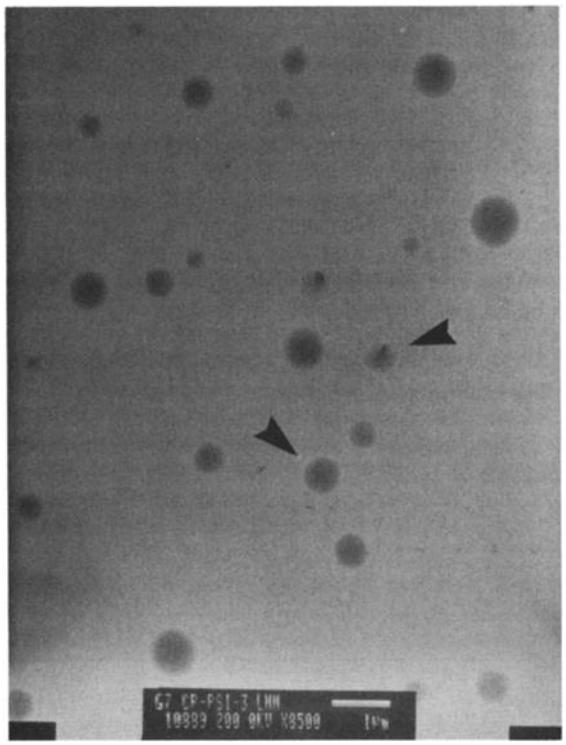

Figure 2. Particles of ammonium sulfate and acidic sulfate collected during the Pacific Sulfur Stratus Experiment (PSI-3). Inclusions are noted within the acidic sulfate particles, identified as sea salt from X ray analysis.

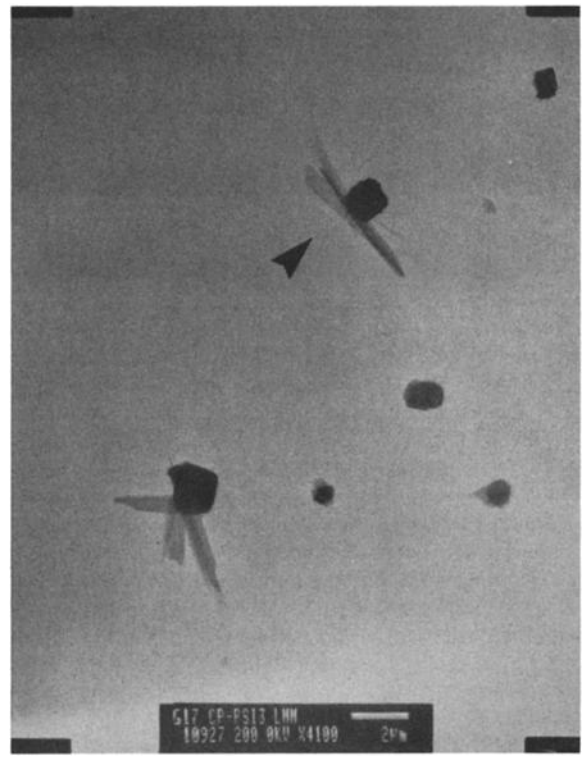

Figure 3. Sea-salt particles with Cl/Na ratios close to bulk seawater collected during PSI-3.

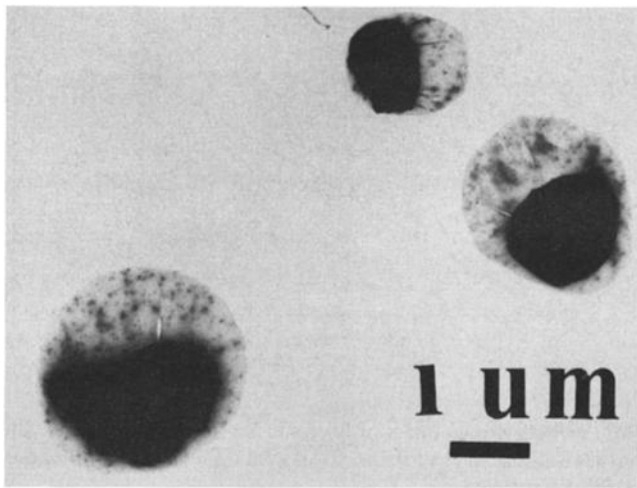

Figure 4a. Acidic sea-salt particles collected at the 12°S station during the International Global Atmospheric Chemistry Program's Marine Aerosol and Gas Exchange Pacific experiment (IGAC MAGE).

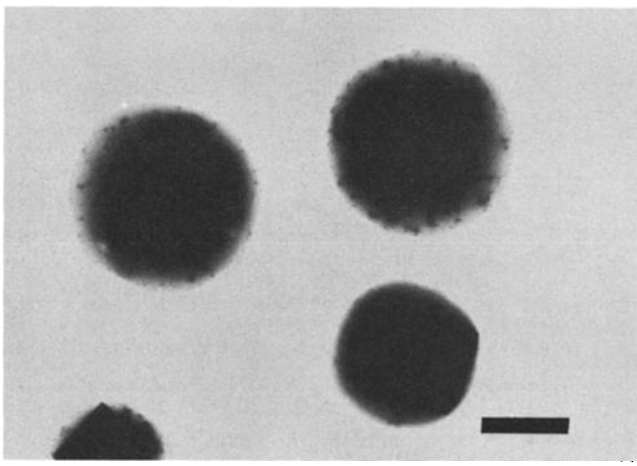

Figure 4b. Sea-salt particles with S/Na ratios higher than bulk seawater and the sea salts shown in Figure 4a.

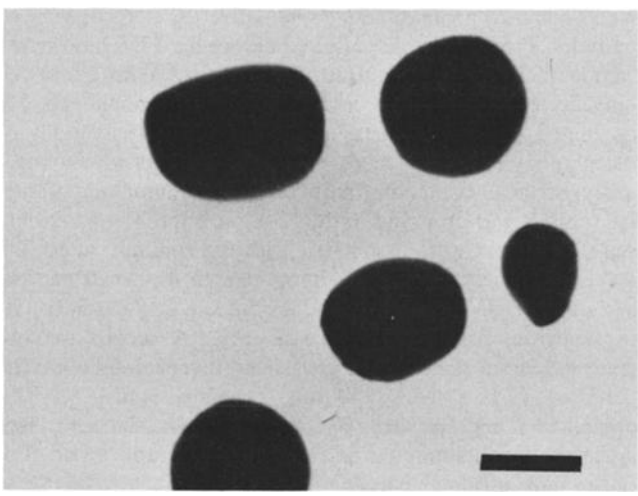

Figure 4c. Sea-salt particles collected at the 12°S station during IGAC MAGE. The S/Na ratios are higher than bulk seawater and the sea salts shown in Figure 4b. As well, the Cl/Na ratios are lower than bulk seawater.

ratios of Cl/Na, selected area analysis of the cubic portion of the particle provided the best calibration results, $R^2 > 0.98$. The calibration curve for Cl/Na shown in Figure 9 represents the combined results from selected area analysis and whole area analysis for artificial sea-salt and sodium chloride particles. The estimated Cl/Na ratios agree within 10% for both calibration sets. Ion chromatography analysis determined the actual weight ratios of the bulk solutions and filters which concurrently collected the generated aerosols used for the calibrations. No chemical fractionation of these major ions was observed between the generated aerosols and the parent solution. Table 3 summarizes the weight ratios measured by ion chromatography for the calibration sea-salt particles as well as reported values for bulk seawater.

The aerosols collected during the time series stations at 12°S and 2°S on the MAGE cruise were also analyzed by EDX. In most of the sodium-containing particles, additional sea-salt cations were detectable. Due to instrumental detection limits, sea-salt cations were not detected in sea-salt-containing particles of 0.10 μm or less; only the Na and S were consistently seen in these particles. Examination of elemental ratios obtained by whole area analysis (Figures 10a, 10b, and 10c), revealed 96% of the Ca/Na, 87% of the K/Na, and 86% of the Mg/Na ratios fell within the confidence intervals (double-tailed t test, 99.9%) of the reference bulk seawater value for the particles examined. The S/Na and Cl/Na ratios (Figures 10d and 10e) show significant deviation from the reference value, with 98% and 70% of the particles falling outside the confidence interval. This deviation and range in measured ratios reflects the extent of chemical reaction of $H_2SO_4(g)$ occurring in the atmosphere. The relationship between the molar ratios of Cl/Na and nss S/Na is shown in Figure 11.

It is interesting to note that for many particles the S/Na molar ratio exceeded 0.59, the molar ratio of sea-salt NaCl fully reacted with sulfate. Additional base would be required

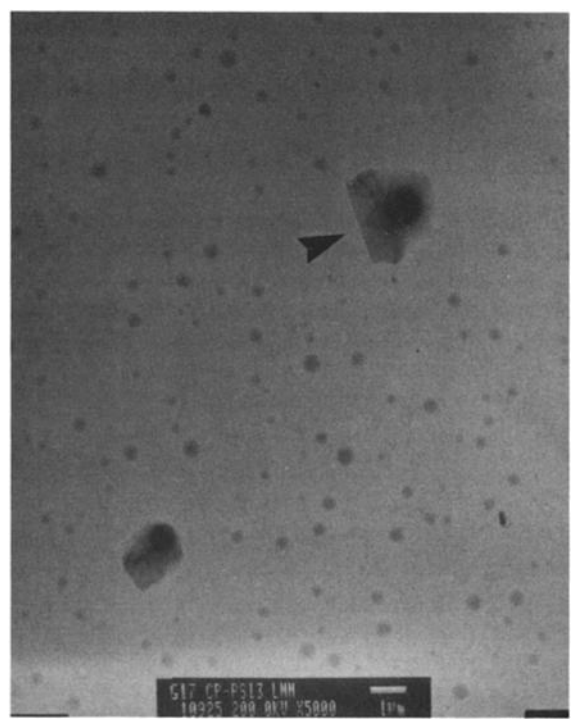

Figure 5. The submicrometer particles are ammonium sulfate; the larger ones are sea-salt particles which contain excess S. The particles were collected during PSI-3.

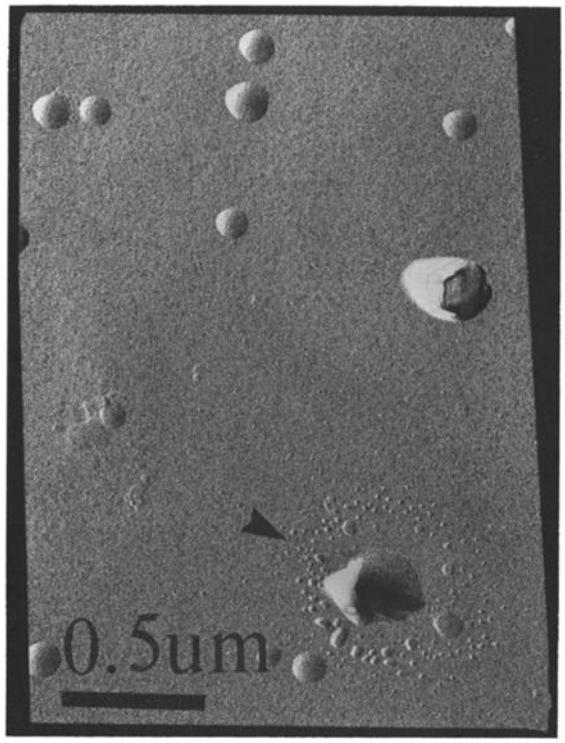

Figure 6. Acidic sea-salt particle and ammonium sulfate particles collected at the 12°S station during IGAC MAGE. The sample has been shadow coated with Au Pd.

for the uptake and oxidation of $SO_2(g)$ to raise the ratio above 0.59, since its solubility is pH dependent. Vapor deposition of sulfuric acid onto preexisting particles is not pH dependent, however. Since the calibration has not been extended for particles greater than 1.0 μm in diameter, the results for the particles greater than this size should be considered with caution. If we assume the calibration factor for the Cl/Na ratio is the same as or reasonably close to that measured for the laboratory particles of 0.50 μm, then 48% of the coarse sea-salt particles examined would have chloride chemistry similar to bulk seawater composition. The remaining coarse particles, like those in Figure 4c, contain no Cl or significantly reduced amounts of Cl and additional sulfur. Their morphology, which was not typical of sea salt, coupled with EDX information, indicates that these particles are chemically more like sodium sulfate or sodium sulfate with $SO4^{2-}$/Na ratios in excess of 0.59.

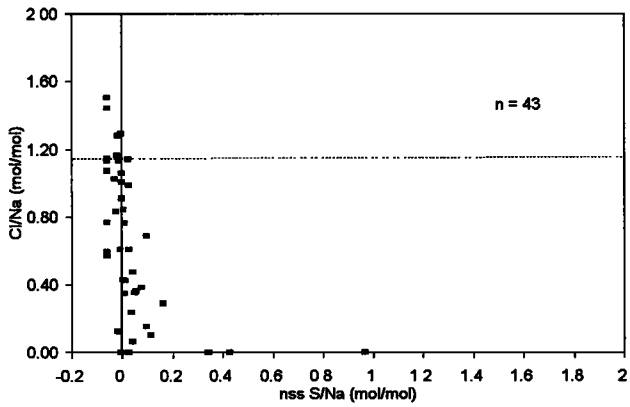

Figure 7. Mole ratio of Cl/Na to nss S/Na for sea-salt containing particles collected during PSI-3. Seawater reference value indicated.

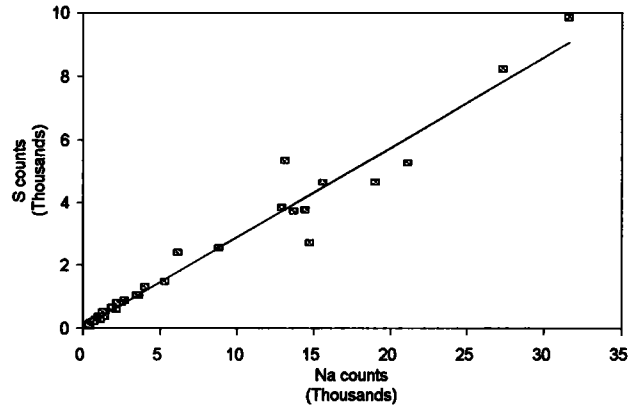

Figure 8a. X ray counts of S versus Na for laboratory-generated sea-salt particles of 0.15-, 0.25-, and 0.50-μm Dp; y = 0.286x + 29, R^2 = 0.964.

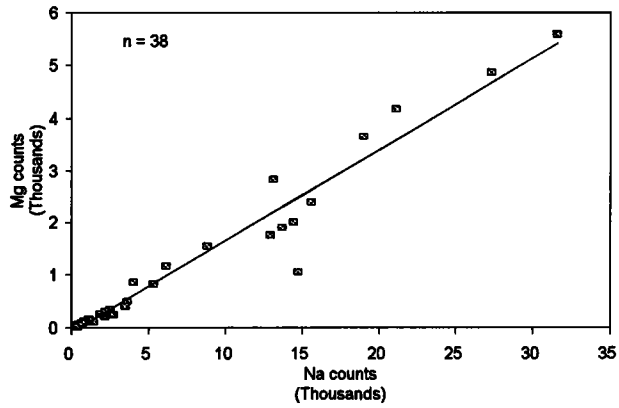

Figure 8b. X-ray counts of Mg vs Na for laboratory generated seasalt particles of 0.15, 0.25, 0.50 um Dp. y = 0.174x - 87 R squared = 0.952

Figure 8b. X ray counts of Mg versus Na for laboratory-generated sea-salt particles of 0.15-, 0.25-, and 0.50-μm Dp; y = 0.174x – 87, R^2 = 0.952.

Estimates of the abundance of sodium-containing particles were obtained from random qualitative X ray analysis of particles. From a sample collected during the 12°S time series station, 89% of the particles ($0.15 \leq Dp \leq 0.50$ μm) contained only S, 9% contained S and Na, while the remaining 2% contained S, Na, and measurable Cl. From observations of morphology and inferences from size-segregated chemical analysis, the S-containing particles were ammonium sulfate, i.e., only S was observed in the X ray spectra. The additional sea-salt cations were associated with the sodium, unless the levels were below detection limits due to the small particle sizes analyzed. The uncertainty attributable to Poisson counting statistics for 50 particles was 14%. A second random analysis for a sample collected later revealed 69% of the particles ($0.10 \leq Dp \leq 0.50$ μm) contained only S, 23% contained S and Na, and 8% contained S, Na, and Cl . Here again the S-containing particles were ammonium sulfate. The uncertainty attributable to Poisson counting statistics was 20%.

Chemical analysis of cascade impactor samples was done by ion chromatography for the PSI-3 experiment [*Quinn et al.*, 1993] and for IGAC MAGE. No measurements of chloride were made for the samples collected during PSI-3. The results from IC analysis of impactor samples collected during the

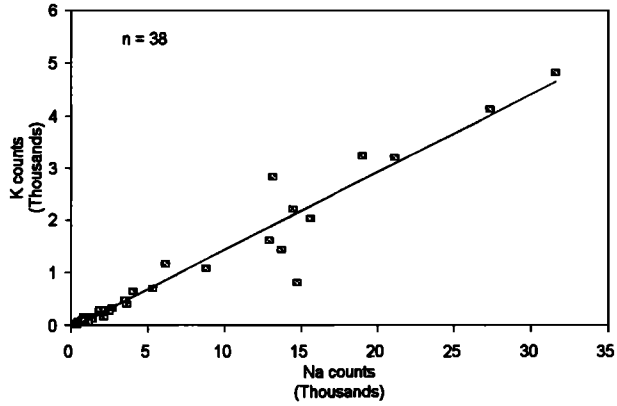

Figure 8c. X ray counts of K versus Na for laboratory-generated sea-salt particles of 0.15-, 0.25-, and 0.50-μm Dp; y = 0.125x − 58, R^2 = 0.974.

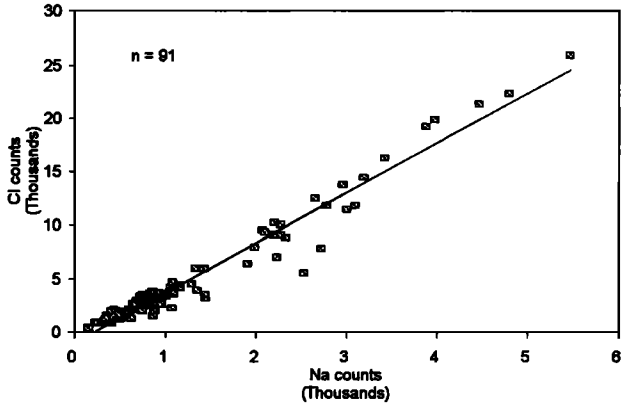

Figure 9. X ray counts of Cl versus Na for laboratory-generated sea-salt particles of 0.15-, 0.25-, and 0.50-μm Dp; y = 4.685x − 1020, R^2 = 0.955.

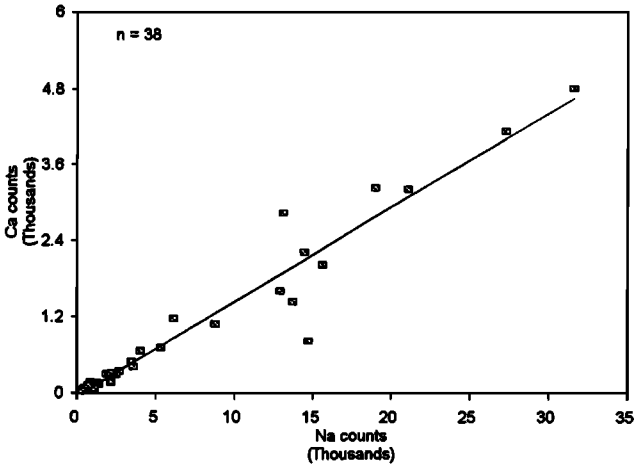

Figure 8d. X ray counts of Ca versus Na for laboratory-generated sea-salt particles of 0.15-, 0.25-, and 0.50-μm Dp; y = 0.149x − 54, R^2 = 0.940.

IGAC MAGE time series station at 12°S (Figure 12a, 12b, and 12c) were examined for the corresponding molar ratios of Cl/Na and nss SO_4^{2-}/Na. The time required to collect enough sample for chemical analysis was 24 hours or more, while for the TEM grids, collection times were about 30 min (Dp > 2.0 μm). Thus the samples are not strictly comparable but air mass character was consistent during the overall sampling period. Size-segregated chemical analysis did not always detect sodium on the smallest impactor stage (Dp < 0.125 μm), possibly due to instrumental detection limits at 5 ng. In the size ranges where more than 95% of the particles were Na containing, the IC and the EDX analysis can be compared. Examination of the molar ratio of nss SO_4^{2-}/Na for the 1.0 ≤ Dp ≤ 2.0 μm and 2.0 ≤ Dp ≤ 4.0 μm stages for the first three samples collected at 12°S revealed no excess sulfate associated with these size increments which were dominated by sea salt by mass, while the next three samples collected show nss sulfate associated with these sea-salt particles. The ratios ranged from 0.09 to 0.21 (nmol/nmol) and from 0.00 to 0.07 (nmol/nmol) for the smaller and larger size increments. The molar ratio of nss SO_4^{2-}/Na for the 0.50 ≤ Dp ≤ 1.0-μm stage reveals even higher ratios (0.04 to 0.43), but it is not known what percentage of the particles collected on this stage contain sea salt. The molar ratios of Cl/Na for these samples are close to or higher than the ratios in bulk seawater. It has not yet been determined if the chloride enrichment measured on the bulk filters is real or an artifact resulting from the absorption of HCl(g) during the long collection times required for sampling. Measurements of HCl(g) were not made during the experiment.

The fraction of nss sulfate mass (Figure 13) for individual particles sampled in the IGAC MAGE and PSI-3 was estimated from the weight ratios determined from EDX. The values ranged anywhere from 0 to 97%. It can be seen that the fraction of sulfate measured for particles of the same size is highly variable. The particles for IGAC MAGE contained higher fractions of nss sulfate, most likely due to high gas phase sulfate precursor concentrations. The range of weight ratio values reported for 12°S agree with the range of nss SO_4^{2-}/Na values of 0.13 to 3.3 (converted from nss S/Na values) reported by *Mouri and Okada* [1993] for samples collected from the Pacific north of the equator. The variability observed for the Ca/Na ratios for particles collected at 12°S is less than that observed in the Mouri and Okada paper, although the average values are similar. The mass loadings of nss sulfate estimated from modeling results of cloud-processed air from *Hegg et al.* [1992] for individual sea-salt particles of Dp 0.46 μm and 0.80 μm were 6 and 22 fg. These model estimates invoke one cloud pass of 10-min duration. The results from IGAC/MAGE from sea-salt particles of 0.50 μm and 0.80 μm report lower estimates of 216 and 861 fg of nss sulfate and upper estimates of 1422 and 5235 fg of nss sulfate. The results from PSI-3 were lower with sea-salt particles containing at most 18 and 661 fg of nss sulfate for particle sizes of 0.50 μm and 1.0 μm. The lower estimates for particles of this size contain no excess sulfate. The results show that the

Table 3. Weight Ratios of Generated Aerosols and Seawater

Element	Aerosol	Seawater*
Na/Na	1.000	1.000
Cl/Na	1.625	1.810
Ca/Na	0.037	0.038
Mg/Na	0.082	0.129
K/Na	0.045	0.036
S/Na	0.116	0.084

*Reference values obtained from the Handbook of Chemistry and Physics.

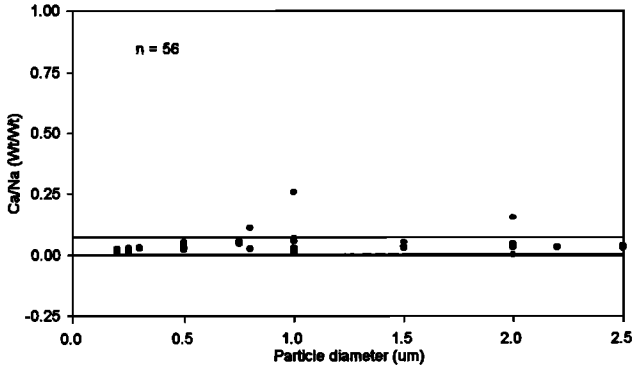

Figure 10a. Variability in the Ca/Na weight ratio for IGAC MAGE particles collected at 12°S. Confidence intervals for reference included at 99.9%.

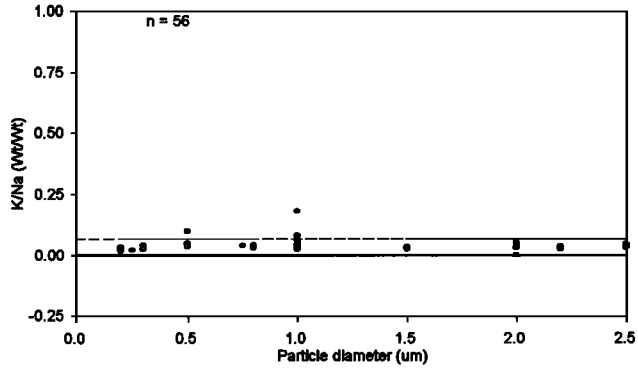

Figure 10b. Variability in the K/Na weight ratio for IGAC MAGE particles collected at 12°S. Confidence intervals for reference included at 99.9%.

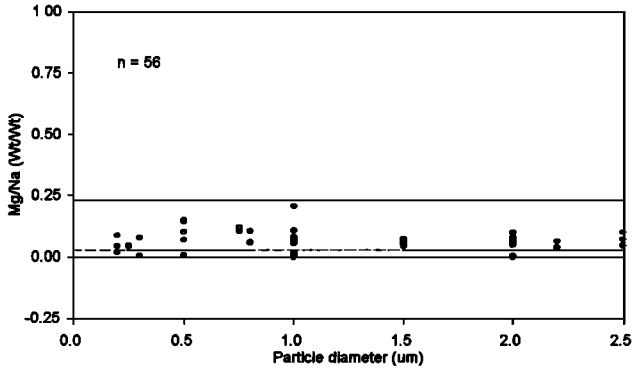

Figure 10c. Variability in the Mg/Na weight ratio for IGAC MAGE particles collected at 12°S. Confidence intervals for reference included at 99.9%.

highest individual sulfate mass loadings per particle were found for particles within the $1.0 \leq Dp \leq 2.5$ μm size range. The molar ratios expected from models simulating S(IV) oxidation in sea-salt aerosol solution droplets were 0.005 S/Na [*Chameides and Stelson*, 1992]. The values we found for individual coarse sea-salt particles were significantly higher than this, which is not unexpected since both processes of sulfuric acid condensation and S(IV) oxidation can occur.

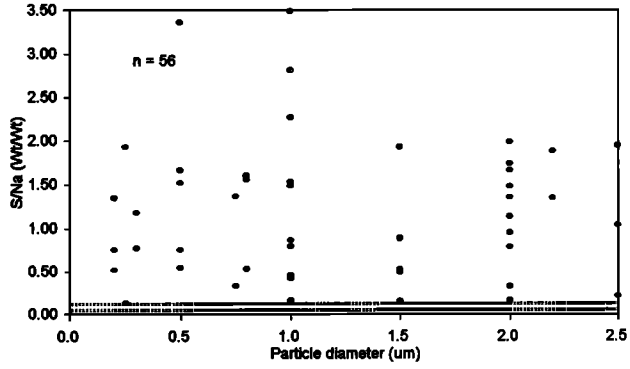

Figure 10d. Variability in the S/Na weight ratio for IGAC MAGE particles collected at 12°S. Confidence intervals for reference included at 99.9%.

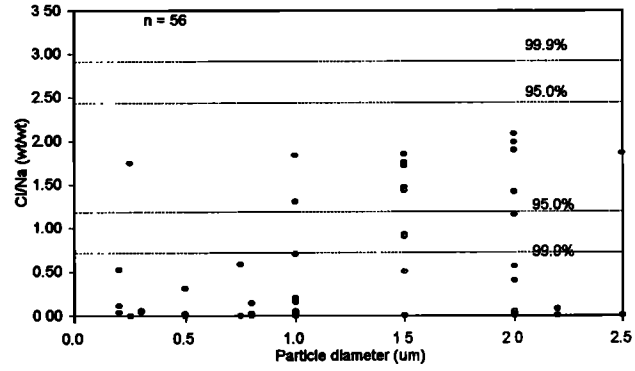

Figure 10e. Variability in the Cl/Na weight ratio for IGAC MAGE particles collected at 12°S. Confidence intervals for reference included at 99.9%.

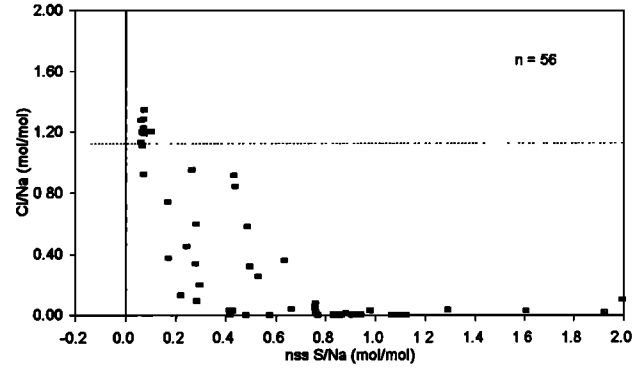

Figure 11. Mole ratio of Cl/Na to nss S/Na for sea-salt-containing particles collected during the stations at 12°S in MAGE 1992. Seawater reference value indicated.

Conclusions

The results obtained from individual sea-salt-containing particles collected in the remote marine boundary layer indicate that most of the submicrometer sea-salt particles from this area are significantly enriched in sulfate. These particles have lost a significant amount of their chloride to the atmosphere where it may be measurable as HCl(*g*) or other inorganic Cl gases [*Pszenny et al.*, 1993]. The S/Na enrich-

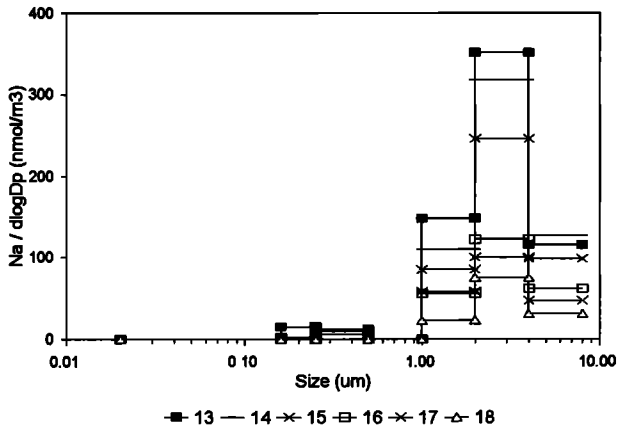

Figure 12a. Ion chromatography (IC) data collected for 12°S for Berner impactor samples.

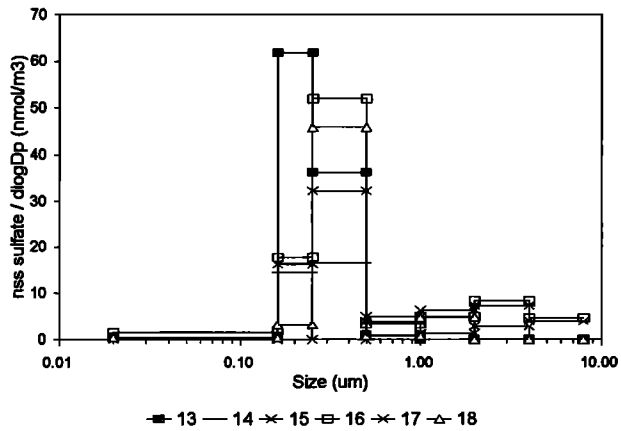

Figure 12b. Ion chromatography (IC) data collected for 12°S for Berner impactor samples.

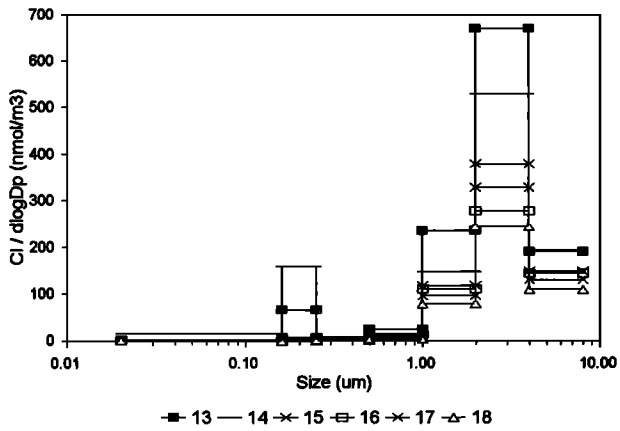

Figure 12c. Ion chromatography (IC) data collected for 12°S for Berner impactor samples.

ment and Cl/Na depletion measured were highly variable even for particles of the same size examined from the same grid sample for both the submicrometer and the coarse sea-salt particles. Above 1 μm some of the sea-salt particles have a chemistry indistinguishable from bulk seawater. However, the larger fraction of these particles show chloride depletion and sulfur enrichment. The weight ratios of Ca/Na, K/Na, and

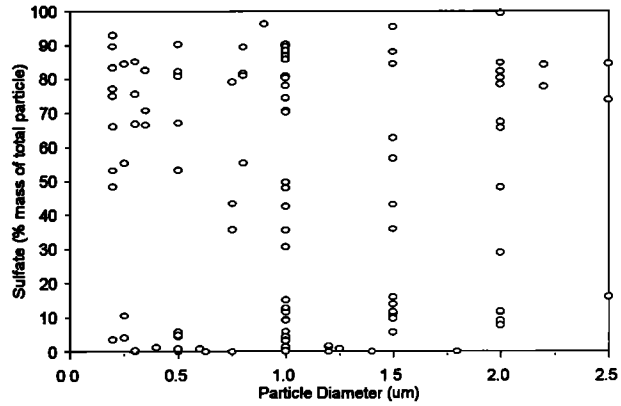

Figure 13. Mass loading of sulfate as a function of particle size for particles collected during IGAC MAGE and PSI-3.

Mg/Na were consistent with sea-salt composition over the size ranges examined. Estimates of nss sulfate mass indicate that collectively, both the submicrometer and the coarse size sea-salt particles contain large fractions of nss sulfate. The highest sulfate to sodium mass ratios occurred in submicrometer particles both individually and collectively, as analyzed by EDX and IC. The highest sulfate mass loadings, on a single-particle basis and collectively (as mass concentrations, g m^{-3}), were found in the supermicrometer mode.

For a subset of particles in the MBL the fractional SO_4^{2-}/Na composition seems to be a continuous variable down to at least particle diameters of 0.1 μm and the detection limits of EDX for Na. Clearly, above these limits the marine aerosol is largely a collection of an externally mixed sulfate aerosol at smaller sizes, an internally mixed aerosol of excess sulfate, and sea-salt of varying proportions over the submicrometer and supermicrometer modes and at larger sizes contains a set of externally mixed sea-salt particles. Considering the sources and transformations of the MBL aerosol mentioned earlier, this chemical size distribution is certainly expected. These results begin to quantify the distribution and provide results to test MBL and tropospheric chemistry models.

The results clearly show that there is not a 1:1 relationship between bulk sodium mass fraction (in sea salt) and the number of sodium-containing particles in the accumulation mode. Sea-salt-containing particles account for a much larger fraction of number than the Na mass fraction would imply. Initial estimates of the abundance of sodium-containing particles within this size range indicate 11 to 33% of the particles are or contain sea salt. Thus sea salt must act as a seed for the uptake and oxidation of sulfur gases and deposition of condensable sulfate vapors. Additional measurements of this type, including single-particle and size-segregated aerosol chemistry analysis, are needed to confirm and extend these results since only two random tests of this type were attempted. Of particular interest is the relationship between the non-sea-salt (nss) sulfate to sodium mass ratio and the total number (N) to the sodium containing (N_{Na}) in both the accumulation and the supermicrometer modes.

Acknowledgments. We thank Don Brownlee and Dave Joswiak for instrumental assistance. This work was funded in part by the Marine Sulfur and Climate project of NOAA's Climate and Global Change Program and the NSF division of Atmospheric Chemistry grants 9311213 and 9008443. This is JISAO contribution 252 and NOAA PMEL contribution 1489.

References

Chameides, W. L., and A. W. Stelson, Aqueous-phase chemical processes in deliquescent sea-salt aerosols: A mechanism that couples the atmospheric cycles of S and sea salt, *J. Geophys. Res., 97*, 20,565–20,580, 1992.

Charlson, R. J., S. E. Schwartz, J. M. Hales, R. D. Cess, J. A. Coakley, Jr., J. E. Hansen, and D. J. Hofmann, Climate forcing by anthropogenic aerosols, *Science, 225*, 423–430, 1992.

Clarke, A., Equatorial convection as a source of tropospheric nuclei over the remote Pacific, paper presented at the First Symposium on Dimethyl Sulfide: Oceans, Atmosphere, Climate, Commision of the Europ. Commun., Belgirate, October 1992.

Cliff, G., and G. W. Lorimer, The quantitative analysis of thin specimens, *J. Microsc., 102*, 203–207, 1975.

Covert, D. S., V. N. Kapustin, P. K. Quinn, and T. S. Bates, New particle formation in the marine boundary layer, *J. Geophys. Res., 97*, 20,581–20,589, 1992.

Eriksson, E., The yearly circulation of chlorine and sulfur in nature: Meteorological, geochemical and pedological implications, *Tellus, 11*, 375–403, 1959.

Ferek, R. J., A. L. Lazrus, and J. W. Winchester, Electron microscopy of acidic aerosols collected over the northeastern United States, *Atmos. Environ., 17*, 1545–1561, 1983.

Frank, E. R., and J. P. Lodge, Morphological identification of airborne particles with the electron microscope, *J. Microsc., 6*(4), 449–456, 1967.

Hegg, D. A., P. Yuen, and T. V. Larson, Modeling the effects of heterogeneous cloud chemistry on the marine particle size distribution, *J. Geophys. Res., 97*, 12,927–12,933, 1992.

Hitchcock, D. R., L. L. Spiller, and W. E. Wilson, Sulfuric acid aerosols and HCl release in coastal atmospheres: Evidence of rapid formation of sulfuric acid particulates, *Atmos. Environ., 14*, 165–182, 1980.

Keene, W. C., A. A. P. Pszenny, D. J. Jacob, R. A. Duce, J. N. Galloway, J. J. Schultz-Tokos, H. Sievering, and J. F. Boatman, The geochemical cycling of reactive chlorine through the marine troposphere, *Global Biogeochem. Cycles, 4*, 407–430, 1990.

Mouri, H., and K. Okada, Shattering and modification of sea-salt particles in the marine atmosphere, *Geophys. Res. Lett., 20*, 49–52, 1993.

O'Dowd, C. D., and M. H. Smith, Physicochemical properties of aerosols over the Northeast Atlantic: Evidence for wind-speed-related submicron sea-salt aerosol production, *J. Geophys. Res., 98*, 1137–1149, 1993.

Parungo, F. P., C. T. Nagamoto, J. Rosinski, and P. L. Haagenson, A study of marine aerosols over the Pacific Ocean, *J. Atmos. Chem., 4*, 199–226, 1986.

Prospero, J. M., D. L. Savoie, R. T. Nees, R. A. Duce, and J. Merrill, Particulate sulfate and nitrate in the boundary layer over the North Pacific Ocean, *J. Geophys. Res., 90*, 10,586–10,596, 1985.

Pszenny, A. A. P., W. C. Keene, D. J. Jacob, S. Fan, J. R. Maben, M. P. Aetwo, M. Springer-Young, and J. N. Galloway, Evidence of inorganic chlorine gases other than hydrogen chloride in marine surface air, *Geophys. Res. Lett., 20*(8), 699–702, 1993.

Quinn, P. K., D. S. Covert, T. S. Bates, V. N. Kaspustin, D. C. Ramsey-Bell, and L. M. McInnes, Dimethylsulfide/cloud condensation nuclei/climate system: Relevant size-resolved measurements of the chemical and physical properties of atmospheric aerosol particles, *J. Geophys. Res., 98*, 10,411–10,427, 1993.

Raemdonck, H., W. Maenhaut, and M. O. Andreae, Chemistry of marine aerosols over the tropical and equatorial Pacific, *J. Geophys. Res., 91*, 8623–8636, 1986.

Raes, F., R. Van Dingenen, J. Wilson, and A. Saltelli, Cloud condensation nuclei from dimethyl sulfide in the natural marine boundary layer: Remote vs in situ production, paper presented at the First Symposium on Dimethyl Sulfide: Oceans, Atmosphere, Climate, Commission of the Europ. Commun., Belgirate, October 1992.

Shaw, G. E., Aerosol chemical components in Alaska air masses, 2, Sea salt and marine product, *J. Geophys. Res., 96*, 22,369–22,372, 1991.

Sievering, H., G. Ennis, and E. Gorman, Size distributions and statistical analysis on nitrate, excess sulfate, and chloride deficit in the marine boundary layer during GCE/CASE/WATOX, *Global Biogeochem. Cycles, 4*, 395–495, 1990.

Sievering, H., J. Boatman, J. Galloway, W. Keene, Y. Kim, M. Luria, and J. Ray, Heterogeneous sulfur conversion in sea-salt aerosol particles: The role of aerosol water content and size distribution, *Atmos. Environ., 8*, 1479–1487, 1991.

Sievering, H., J. Boatman, E. Gorman, Y. Kim, L. Anderson, G. Ennis, M. Luria, and S. Pandis, Removal of sulphur from the marine boundary layer by ozone oxidation in sea-salt aerosols, *Nature, 360*, 571–573, 1992.

Zhou, M. Y., S. J. Yang, F. P. Parungo, and J. M. Harris, Chemistry of marine aerosols over the western Pacific Ocean, *J. Geophys. Res., 95*, 1779–1787, 1990.

D. S. Covert, Joint Institute for the Study of Atmosphere and Ocean, GJ-40, University of Washington, Seattle, WA 98195.

M. S. Germani, McCrone Associates, 850 Pasquinelli Drive, Westmont, IL 60559.

L. M. McInnes, Department of Chemistry, BG-10, University of Washington, Seattle, WA 98195.

P. K. Quinn, NOAA Pacific Marine Environmental Laboratory, 7600 Sand Point Way NE, Seattle, WA 98115.

(Received June 21, 1993; revised October 20, 1993; accepted November 29, 1993.)